Published in final edited form as:
J Porphyr Phthalocyanines. 2011 ; 15(9-10): 918–929. doi:10.1142/S108842461100380X.

Syntheses, properties and cellular studies of metalloisoporphyrins

Sandra C. Mwakwari, **Haijun Wang**, **Timothy J. Jensen**, **M. Graça H. Vicente**◇, and **Kevin M. Smith**[*,◇]
Department of Chemistry, Louisiana State University, Baton Rouge, LA 70803, USA

Abstract

b-Bilene hydrochlorides are shown to be improved intermediates for the synthesis of metallo-isoporphyrins in enhanced yields (28% *vs*. 6%). Several new diamagnetic zinc(II) and a novel paramagnetic copper(II) isoporphyrin salts were also obtained using this approach. Metal-free isoporphyrins were also isolated. *In vitro* studies using human carcinoma HEp2 cells show that all metallo-isoporphyrins accumulate within cells and localize partially in the mitochondria. The zinc-isoporphyrins were found to be moderately phototoxic while the copper complex showed the lowest phototoxicity, maybe as a result of its paramagnetic nature.

Keywords

intracellular localization; metalloisoporphyrins; porphyrins; synthesis; toxicity

Introduction

Isoporphyrins (**1**) are tautomers of porphyrins (**2**) which exhibit interrupted macrocyclic conjugation due to the presence of a saturated (sp^3) bridging carbon atom. They contain three sp^2 and one sp^3 hybridized *meso* carbons and one NH. The existence of this type of compound was first suggested by Woodward [1] in 1961, whose prediction was confirmed about a decade later when Dolphin *et al.* [2] reported the first synthesis of a metalloisoporphyrin (**4**) from zinc 5,10,15,20-tetraphenylporphyrin by way of electrochemical oxidation. Other methods for directly generating metallo-isoporphyrins since then include peroxide oxidation [3, 4] and photooxidation [5–8].

Due to their absorption at long wavelengths (~800 nm), metallo-isoporphyrins are potential candidates as photosensitizers in photodynamic therapy (PDT), a ternary modality for cancer treatment. At long wavelengths, light penetrates deeper through tissue, making it possible to treat large or deep-seated tumors. Metallo-isoporphyrins are also of biological interest due to their unique redox properties among porphyrin derivatives with potential as a new class of near-IR dyes [4, 9–13].

[*]Correspondence to: Kevin M. Smith, kmsmith@lsu.edu, tel:+225-578-7442, fax: +225-578-3458.
◇SPP full member in good standing

Dedicated to Professor Karl M. Kadish on the occasion of his 65th birthday

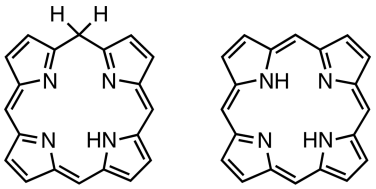

1 2

All early examples of metallo-isoporphyrins were derived from tetraphenylporphyrin metal complexes, and they are usually not stable with regard to reconversion into the corresponding fully conjugated porphyrins [2, 4]. This problem was overcome when Smith and co-workers [14, 15] reported the total synthesis of the first thermodynamically stable zinc isoporphyrin bearing a geminal-dimethyl *meso*-motif; it was prepared using the MacDonald "2+2" method [16]. The availability of this stable zinc isoporphyrin immediately initiated a series of studies on this compound, including electrochemical [17], crystallograpic [18], and photophysical investigations [19].

However, using the MacDonald appraoch, zinc isopoporphyrin products were isolated in low yields. Herein, we report more efficient syntheses of metallo-isoporphyrins from b-bilene salts, and studies of their chemical, physical and biological properties to probe the potential for applicability in photodynamic therapy.

RESULTS AND DISCUSSION

Synthesis of zinc(II) isoporphyrin (6)

The synthetic route investigated involves cyclization of open chain tetrapyrrole intermediates, notably b-bilenes, by ring closure using a suitable carbon-linking unit as the final step.

The precursor b-bilene hydrochloride (**5**) was synthesized by condensation of dipyrromethane-1-carboxylic acid (**3**) [20] with 1-formyldipyrromethane (**4**) to yield crystalline b-bilene hydrochloride in 70% yield; in initial studies this was followed by cyclization using 2,2-dime-thoxypropane as an acetone surrogate and carbon linking unit, then addition of zinc salt to afford the zinc isoporphyrin cation (**6**) in 28% yield (Scheme 1). These yields were higher than previously reported (6%) [14, 15] and the reaction time was dramatically reduced from six days to one day. Other ketones, for example cyclohexanone or the 1,1-dimethoxycyclohexane, proved too bulky for the cyclization reaction.

Synthesis of metal complexes other than zinc(II)

To date, only the zinc(II) isoporphyrin complexes and metal-free derivatives have been isolated [14, 15], and the latter only with difficulty [15]. We are now able to synthesize a copper(II) isoporphyrin in 23% yield; metalation of the metal free isoporphyrin intermediate with cuprous chloride yielded a novel copper isoporphyrin (**7**) (Scheme 1) with an observed bathochromic shift of both the Soret and the Q-band in its optical spectrum (Fig. 1) to 428 and 842 nm (compared with zinc isoporphyrin at 416 and 804 nm). Since the copper(I) salt was used, formation of a neutral copper(I) isoporphyrin complex was expected, but qualitative EPR studies (Fig. 2) confirmed the presence of a paramagnetic copper(II) species, a copper(II) cationic isoporphyrin complex with a chloride counterion. As expected, ^{1}H NMR spectroscopy of this compound in $CDCl_3$ showed no signals for the macrocycle; the product was therefore characterized using spectrophotometry and low resolution/high resolution mass spectrometry. Though the analysis confirmed that the metal complex was copper(II), attempts to synthesize the copper isoporphyrin using copper(II)

salts were unsuccessful. In addition, attempts to obtain other metal complexes using $CuCl_2$, $Ni(acac)_2$, $FeCl_2$, AgCl, and $CdCl_2$ salts, failed.

Synthesis and characterization of metal-free isoporphyrins

It is known that metal-free isoporphyrins are not very stable [15], and therefore no such isoporphyrins have ever been fully isolated and characterized. Two approaches have previously been attempted to obtain a metal-free isoporphyrin: (i) direct synthesis utilizing a variation of the MacDonald 2+2 procedure, and (ii) demetalation of stable zinc isoporphyrins [14, 15]. However, the expected metal-free isoporphyrin could not be isolated and although demetalation was successful, following several trials the product was unstable and decomposed readily. Utilizing the already developed b-bilene synthetic route, the metal-free compound was directly synthesized by cyclization of b-bilene hydrochloride (**5**) in the presence of zinc acetate with 2,2-dimethoxypropane as the carbon-linking unit at room temperature in the presence of air. After 24 hours, the UV-visible spectrum of the reaction mixture showed absorption peaks at 420 and 700 nm, characteristic of metal-free isoporphyrin. Attempts to purify and characterize the compound remained challenging because of product decomposition. Being aware of previous reports of decomposition in the presence of sodium bicarbonate, working under basic conditions was avoided, and successful purification of the compound was performed on an alumina chromatography column using acid treated solvents for elution. It was discovered that the metal-free complex was relatively stable under acidic conditions. Scheme 2 shows the synthesis of the protonated metal-free complex (**8**) obtained as a green compound in 23% yield, with absorptions at 432 nm and 700 nm (Fig. 3).

Mass spectrometry confirmed the formation of the metal-free product (**8**) but, as had previously been observed [15], ^{1}H NMR spectroscopy showed all expected signals except for the 5,5-dimethyl protons (expected to appear between 1–2 ppm) plus a strong (impurity?) signal at 1.26 ppm which did not integrate to the expected 6-methyl protons. The missing signal was assumed [15] to be obscured beneath the impurity peak at 1.26 ppm. The missing signal was also initially associated with some unusual dynamic processes which was ruled out after performing a variable-temperature ^{1}H NMR study. To locate the missing NMR signal, a deuterium labeling strategy of the 5,5-dimethyl substituents by chemical synthesis was employed. This was achieved by cyclizing the b-bilene hydrochloride (**5**) with acetone-d_6 as the carbon-linking unit to introduce deuterium into the macrocycle (Scheme 2). It was necessary to ensure that the reaction conditions did not allow D/H isotopic exchange by carrying out the synthesis using TFA-d and acetone-d_6. The reaction was followed by spectrophotometry and after 24 h the characteristic absorption peak at 700 nm was at its maximum. Purification on neutral alumina and silica gel under acidic conditions provided the green target deuterium-labeled compound (**9**). Using ^{1}H NMR spectroscopy of this sample in chloroform-d the signal at 1.26 ppm was still present, with the same intensity as in the spectrum of compound (**8**).

Solvent stability studies were performed [21] on the deuterated product and the NMR studies were carried out in a different solvent hoping to obtain better solubility and resolution. The solvent of choice was acetone-d_6 containing a trace of TFA-d to stabilize the metal-free isoporhyrin (**8**). In this solvent, a signal at ~1.7 ppm which integrated to 6-H was observed, this corresponding to the 5,5-dimethyl protons. To confirm the identity of this signal, the deuterium labeled metal-free isoporphyrin (**9**) was analyzed under the same conditions by ^{1}H NMR in acetone-d_6 and the signal was absent. Another observation made was the reduced intensity of the signal at 1.26 ppm in acetone-d_6 compared with chloroform-d, possibly due to better solubility/reduced aggregation in the acetone/TFA mixture and stability of the metal-free macrocycle in this solvent mixture. To further verify the structure

of metal-free isoporphyrin and to confirm presence and location of the 5,5-dimethyl protons, more sensitive ^{13}C NMR techniques (DEPT 135 and DEPT 90) were employed. The metal-free macrocycle, which has symmetry through the 5,15-*meso*-positions, would be expected to yield positive signals corresponding to 2-CH carbons in DEPT 90, while positive 2-CH carbons and 5-CH_3 carbons in DEPT 135, for non-deuterated metal-free isoporphyrin. On the other hand, deuterium labeled metal-free isoporphyrin would be expected to show positive signals for 2-CH carbons in DEPT 90, and positive 2-CH carbons and 4-CH_3 carbons in DEPT 135, due to deuterium labeling of the 5,5-dimethyl motif. Both samples were dissolved in $CDCl_3$ and four different experiments were run overnight to obtain results which complied precisely with the theoretical speculations/predictions. These results confirmed the location of the 5,5-dimethyl signal at 1.70 ppm in acetone and 1.26 ppm in chloroform.

Synthesis of *meso*-monosubstituted porphyrins *via* isoporphyrins

In an attempt to further improve the yield of the b-bilene cyclization step to give isoporphyrins, linking carbon units other than those related to acetone were investigated. Cyclization of b-bilene salts with α-ketoesters and α-diketones afforded new isoporphyrin macrocycles. The isoporphyrins from the α-ketoesters (e.g. **10d**) were subsequently transformed with KOH in methanol into the corresponding zinc(II) *meso*-monosubstituted porphyrins, and after demetalation into the *meso*-substituted free-base porphyrin (**11d**; Scheme 3). Figure 4 shows the absorption spectral changes as zinc(II) isoporphyrin (**10d**) was transformed *via* the zinc(II) complex into metal-free *meso*-substituted porphyrin (**11d**).

During the macrocyclization process (Scheme 3), a novel transformation from b-bilene through a,b-biladiene to a,c-biladiene was observed; for a preliminary publication of this work see [22]. Use of these new α-di-carbonyl linking units resulted in significant improvements in the yields of isoporphyrins obtained.

Table 1 shows the various α-ketoesters (entries **a**–**f**) and the α-diketone (entry **g**) used in the b-bilene cyclization reactions to afford the corresponding zinc isoporphyrin cation complexes in yields (33–56%) significantly higher than previously reported [14, 15]. The reactions were carried out at room temperature and were complete in about one hour depending upon the carbonyl substrate. The high electrophilicity of the carbonyl on the α-ketoesters and α-diketone substrates compared with simple ketones (such as acetone) facilitated the enhanced rate of the reaction. The results indicate that the more bulky is the substrate the lower is the yields of isoporphyrin. Surprisingly (Table 1, entry **c**), no cyclization occurred with methyl 3,3,3-trifluoromethylpyruvate to give zinc isoporphyrin, despite the highly electrophilic character of the carbonyl due to the presence of the electronegative fluorine atoms. For entry (**f**), steric factors may have played a role in the lack of cyclization.

Having successfully synthesized a library of target zinc(II) isoporphyrins (**10**), their potential as intermediates in the synthesis of *meso*-substituted porphyrins was studied. Saponification of the 5-alkyl ester substituent to give carboxylic acid followed by decarboxylation on the sp^3-hybridized *meso* carbon led to a rapid transformation of the cationic complex into the corresponding zinc(II) *meso*-monosubstituted porphyrin, which was then demetalated to give **11d** in 32% yield, (Scheme 3). 10% KOH dissolved in dry methanol was used for this reaction. It was discovered that when KOH was dissolved in water the reaction did not proceed as expected. The reaction occurred at room temperature and formation of the product was monitored by spectrophotometry, monitoring the Soret band of the product (around 400 nm) until it reached its maximum intensity. Purification was performed on an alumina (Grade III) column. The driving force for the decarboxylation reaction is the considerable thermodynamic stabilization gained upon the formation of a

fully conjugated isomer (porphyrin **11**) in comparison to zinc isoporphyrin (**10**) that exhibits an interrupted macrocyclic conjugation owing to the presence of a sp^3-hybridized *meso* carbon. Subsequent attempts to functionalize/conjugate the geminal ester function (for example with amino acids), *via* the alkyl ester, have been thwarted by this facile decarboxylation after hydrolysis, and attempts to circumvent this process are in progress.

Owing to the success of the methodology whereby zinc metal was incorporated into the intermediate before cyclization and oxidation to zinc isoporphyrin, it was speculated that incorporation of other transition metals may allow for the isolation of metallo-isoporphyrins that may otherwise be inaccessible by direct metalation of metal-free macrocycles. Several transition metal salts including CuCl, $CuCl_2$, $Ni(acac)_2$, Fe(II), Co(II), Ag(I), Cd(II), were incorporated into the intermediate followed by addition of DDQ at room temperature with no successful cyclization to the corresponding metallo-isoporphyrin. Mostly, decomposed products were obtained (monitored by UV-vis spectroscopy).

Cellular studies

Figure 5 shows the results of time dependent cellular uptake of zinc-isoporphyrins **6, 10a, 10b, 10d,** and **10e**, investigated in HEp2 cells at a concentration of 20 μM over a time period of 24 h. All the compounds exhibited a rapid uptake within the first 2–4 h. Compounds **6** and **10d** reached a plateau after 4 or 8 h, respectively, while all other compounds continued to accumulate within cells during the 24 h period investigated. Among the zinc-isoporphyrins studied, compounds **10d** and **10e** accumulated the most within cells at all time points, and after 24 h the amount of **10e** found in cells was twice that found in **10a** and about 5-fold that of **6**. It is interesting to note the significant differences observed in the cellular uptake of this series of structurally similar isoporphyrins; in particular, the presence of a bulky group at the tetrahedron carbon, such as an isobutyl (as in **10e**) or phenyl (as in **10d**) rather than a methyl as in all other compounds, enhanced cellular uptake, probably due to decreased aggregation.

The dark and phototoxicity assays of isoporphyrins **6**, **7**, **10a**, **10b**, **10d**, and **10e**, in HEp2 cells at increasing concentrations of up to 100 μM were evaluated and the results obtained are summarized in Table 2. All metal-lo-isoporphyrins, especially the copper isoporphyrin **7**,showed low dark toxicities. The IC_{50} value, which defines 50% cell viability, for the dark toxicity of the copper isoporphyrin was the highest found among all isoporphyrins, 85 μM (Table 2). On the other hand, the zinc isoporphyrins generally showed higher cytotoxicities, especially upon light activation (~1 J/cm^2 light dose); the most phototoxic was zinc-isoporphyrin **10e**, probably as a consequence of its high cellular uptake (Fig. 5) and multiple sites of intracellular localization (Table 2). These results reflect the profound effect of the nature of the metal ion on the macrocycle. It is to be expected that the zinc-isoporphyrins will be more efficient than the copper complexes at generating singlet oxygen upon light activation, due to the paramagnetic nature of the d^9 Cu(II) ion compared with the diamagnetic d^{10} Zn(II) complexes. Observation of PDT activity in copper tetrapyrroles is unusual but not unique [23, 24].

The intracellular localizations of zinc-isoporphyrins (**6**, **7**, **10a**, **10b**, **10d**, and **10e**) were investigated in HEp2 cells using fluorescence microscopy. The organelle-specific fluorescent probes ERtracker Green (ER), Lysotraker Green (lysosomes), Mitotracker Green (mitochondria) and BODIPY Ceramide (golgi) were used in overlay experiments. The results obtained are shown in Figs 6–10 and Table 2. Our results indicate that all metallo-isoporphyrins localize to some extent in cell mitochondria, a critically important organelle and PDT target [25]. Such mitochondrial localization might be favored for these hydrophobic and cationic molecules for reasons that have been previously observed [25, 26].

Cationic compounds tend to accumulate in the mitochondria in part due to the highly negative electro-chemical potential of the inner mitochondrial system. Mitochondrial localization is important because porphyrin-induced apoptosis in tumors has been correlated with mitochondrial photodamage, and usually occurs rapidly as a result of a cascade-like cell killing process, leading to a rapid loss of treated tissue [27, 28]. On the other hand, the most phototoxic compounds were those that were found in multiple organelles, in addition to mitochondria, specifically in Golgi, lysosomes and ER. Photodamage to organelles other than mitochondria has also been shown to lead to apoptotic pathways [29]; therefore photodamage to multiple organelles might trigger several apoptotic pathways that induce effective cell destruction.

EXPERIMENTAL

Materials

All commercially available starting materials were used without further purification. Solvents were purified and dried from a specially designed solvent purification system from Innnovative Technology, Inc. Analytical TLC using Sorbent Technologies 200 μm silica gel or alumina neutral plates with UV 254 was used to monitor all reactions. E. Merck neutral alumina (70–230 mesh) either deactivated with 6% water (grade III) or non- deactivated (grade 0) and Merck silica gel 60 (70–230 mesh) were used for column chromatography. ^{1}H NMR spectra were obtained on a Bruker DPX-250, Bruker ARX-300, and Bruker DPX-400 spectrometers. Chemical shifts (δ) are given in ppm. Electronic absorption spectra were measured on PerkinElmer Lambda 35 UV/VIS Spectrometer. Low and high resolution mass spectra were obtained on a Bruker ProFlex III MALDI-TOF and Hitachi M8000 ESI mass spectrometer. The compounds were dissolved in dichloromethane or chloroform using dithranol as the matrix and in acetonitrile for HR-ESI. The EPR data were acquired on Bruker WinEPR.

Syntheses

Di-*tert*-butyl 2,3,7,8,12,13,17,18-octamethyl-b-bilene hydrochloride (5)—50 mg (0.14 mmol) of dipyrromethane monocarboxylic acid (**15**) and formyldipyrromethane (**16**) (40 mg, 0.12 mmol) were dissolved in 10 mL of dry dichloromethane and stirred under argon. *p*-toluenesulfonic acid (53 mg, 2 equiv.) was added in two portions to the solution and stirring was continued for 2 h, after which TLC showed no starting material and the UV-visible spectrum showed a strong absorption at 502 nm. The dark red solution was washed with 5% sodium carbonate solution and water and dried over magnesium sulphate. Evaporation of solvent under reduced pressure afforded the tetrapyrrolic intermediate (b-bilene). The dark residue was then dissolved in 5 mL dichloromethane and hydrogen chloride gas was bubbled through the yellowish-orange solution for 10 s; the color changed to dark red, forming the hydrochloride salt. Immediately, the solvent was evaporated and the residue was taken up twice in dry toluene and evaporated in order to remove any traces of water and HCl. The residue was recrystallized from DCM/hexane and left in the freezer overnight. Filtration of solvent yielded orange-red prisms of the b-bilene hydrochloride (**5**) (54 mg, 70%). mp > 300 °C (dec). UV-vis (CH_2Cl_2): λ_{max}, nm (ε × 10^5, M^{-1} cm^{-1}) 502 (1.11). ^{1}H NMR ($CDCl_3$, 250 MHz): δ, ppm 13.8 (br, NH^+, 2H), 10.4 (br, NH, 2H), 7.08 (1H), 4.2 (CH_2, 4H), 2.23, 2.18, 2.04, 2.02, (each CH_3, 6H), 1.55 (*t*-butyl, 18H). HRMS (MALDI-TOF): calcd. for $C_{37}H_{50}N_4O_4$ 614.3827, found *m/z* 614.3832 $[M]^+$.

Zinc(II) 2,3,5,5,7,8,12,13,17,18-decamethylisoporphyrin chloride (6)—Without further purification, the bilene (**5**) (50 mg, 0.08 mmol) was dissolved in 0.2 mL of cold TFA in a round bottomed flask and stirred for 10 min under argon. The mixture was diluted with dry dichloromethane followed by addition of zinc(II) acetate (50 mg) dissolved in dry

methanol (2 mL), and excess 2,2-dimethoxy propane. The mixture was left to stir in air for 28 h. TLC and UV-visible showed formation of product. The electronic absorption spectrum showed peaks at around 440 and 690 nm characteristic of metal-free isoporphyrin. Work-up was caried out by washing with water twice, drying over anhydrous Na_2SO_4 and evaporating the solvent. The residue was immediately dissolved in dichloromethane and zinc(II) acetate in methanol was added. After 15 min, the absorption spectrum showed successful insertion of zinc ions with absorptions red shifted to 810 nm. The product was chromatographed on a silica gel column, eluting with 1–3% methanol/dichloromethane. The appropriate fractions were collected and the solvent was removed. The product was dissolved in dichloromethane, washed with saturated sodium chloride solution and dried over Na_2SO_4. Recrystallization using dichloromethane/petroleum ether afforded the product as a green solid (12 mg, 28%). mp > 300 °C (dec); Lit[15]. >300 °C (dec.). UV-vis (CH_2Cl_2): λ_{max}, nm ($\varepsilon \times 10^3$, $M^{-1}.cm^{-1}$) 420 (48.9), 807 (47.5). ^1H NMR ($CDCl_3$, 300 MHz): δ, ppm 7.70 (s, *meso*-H, 1H), 7.60 (s, *meso*-H, 2H), 2.47, 2.43 (s, β-CH_3, 24H), 1.96 (s, 5-CH_3, 6H). HRMS (MALDI-TOF): calcd. for $C_{30}H_{33}N_4Zn$ 513.1996, found *m/z* 513.1990 $[M]^+$. MS (MALDI-TOF): calcd. 514.999, found *m/z* 514.868 $[M]^+$ (dithranol).

Copper(II) 2,3,5,5,7,8,12,13,17,18-decamethylisoporphyrin chloride (7)—In a round-bottomed flask equipped with a stirrer under argon, was added 50 mg (0.08 mmol) of b-bilene (**5**) and 0.2 mL of cold TFA. The mixture was left to stir for 10 min, after which dry dichloromethane (20 mL) was added followed by an excess of zinc(II) acetate dissolved in dry methanol, then excess 2,2-dimethoxypropane. The reaction mixture was left to stir in air for 24 h. UV-visible (abs. at 700 nm) and TLC on alumina indicated completion of reaction. Excess TFA and dichloromethane were removed by evaporation and the mixture was purified on a column of neutral alumina using acidic solution of chloroform as eluant (two drops of TFA were added to 200 mL of chloroform) to collect a fraction of mixed isoporphyrin and porphyrin. A second column using silica gel and chloroform/ethylacetate 4:1 and a few drops of TFA was performed to separate the isoporphyrin from the porphyrin. The pure isoporphyrin was metalated using excess cuprous chloride in chloroform at room temperature for 2 h. The mixture was filtered through a Celite plug, and the product was crystallized from chloroform/petroleum ether to give the title compound in 23% yield (10 mg). mp > 300 °C (dec). UV-vis (CH_2Cl_2): λ_{max}, nm ($\varepsilon \times 10^3$, $M^{-1}.cm^{-1}$) 428 (10.98), 842 (9.75). HRMS (MALDI-TOF): calcd. for $C_{30}H_{33}CuN_4$ 512.2001, found *m/z* 512.2006 $[M]^+$. MS (MALDI-TOF): calcd. 513.155, found *m/z* 513.339 $[M]^+$ (dithranol).

2,3,5,5,7,8,12,13,17,18-Decamethylisoporphyrin (8)—b-Bilene hydrochloride (**5**) (50 mg, 0.08 mmol) was dissolved in 0.2 mL of cold TFA in a round-bottomed flask and stirred for 10 min under argon. The mixture was diluted with dry dichloromethane followed by addition of zinc(II) acetate (20 mg) dissolved in dry methanol (0.3 mL) and 0.1 mL of 2,2-dimethoxy propane (excess). The mixture was left to stir in air for 24 h. TLC and spectrophotometry showed formation of the product. The electronic absorption showed peaks at around 440 and 690 nm characteristic of a metal-free isoporphyrin. Excess TFA and solvent were evaporated to dryness. The product was chromatographed on a neutral (Brockmann Grade 0) alumina column (approximately two inches long), prepared and eluted with slightly acidified chloroform ($CHCl_3$/TFA: pH= 4–5) to collect the major green fraction. The solvent was evaporated to dryness and dried under vacuum to yield 28% (10 mg) of the target compound. UV-vis (CH_2Cl_2): λ_{max}, nm 432, 700. ^1H NMR ($(CD_3)_2CO$, 300 MHz): δ, ppm 8.43 (s, *meso*-H, 2H), 7.50 (s, *meso*-H, 1H), 2.86, 2.77, 2.61, 2.49 (s, β-CH_3, 24H), 1.64 (s, 5-CH_3, 6H). ^{13}C DEPT 90 ($CDCl_3$, 300 MHz) δ, ppm 106.38, 84.20. ^{13}C DEPT 135 ($CDCl_3$, 300 MHz): δ, ppm 106.38, 84.20, 28.29, 13.06, 11.26, 11.14, 10.79. HRMS (MALDI-TOF): calcd. for $C_{30}H_{36}N_4$ 452.2929, found *m/z* 452.2875 $[M]^+$ (dithranol). MS (MALDI-TOF): calcd. 452.61, found *m/z* 452.59 $[M]^+$ (dithranol).

5,5-Di(trideuteromethyl)-2,3,7,8,12,13,17,18-octamethylisoporphyrin (9)—b-Bilene hydrochloride (**5**) (50 mg, 0.08 mmol) was dissolved in 0.2 mL of cold TFA-d in a round-bottomed flask and stirred for 10 min under argon. The mixture was diluted with dry dichloromethane (20 mL) followed by addition of zinc(II) acetate (20 mg) dissolved in dry methanol (0.3 mL) and 0.07 mL of acetone-d_6 (excess). The rest of the procedure is similar to that described above for compound (**5**).The solvent was evaporated to dryness and the residue dried under vacuum to yield 22% (8 mg) of the target compound. UV-vis (CH_2Cl_2): λ_{max}, nm 429, 692. ^{1}H NMR ($CDCl_3$, 300 MHz): δ, ppm 8.19 (s, *meso*-H, 2H), 7.33 (s, *meso*-H, 1H), 2.80, 2.72, 2.59, 2.47 (s, β-CH_3, 24H). ^{2}H NMR ($CHCl_3$, 300 MHz): δ, ppm 1.85. ^{13}C DEPT 90 ($CDCl_3$, 300 MHz): δ, ppm 106.383, 84.204. ^{13}C DEPT 135 ($CDCl_3$, 300 MHz): δ, ppm 106.33, 84.20, 13.06, 11.26, 11.14, 10.79. HRMS (MALDI-TOF): calcd. for $C_{30}H_{30}D_6N_4$ 458.3299, found *m/z* 458.3262 $[M]^+$ (dithranol). MS (MALDI-TOF): calcd. 458.6, found *m/z* 456.9 ($M\text{-}D^+$) (dithranol).

General procedure for cyclization of b-bilene with dicarbonyl compounds (10)—Cold TFA (0.2 mL) was added to 50 mg (0.08 mmol) of b-bilene hydrochloride (**5**) in a 50 mL round-bottomed flask and left to stir under argon for 10 min. The mixture was diluted with dry dichloromethane (20 mL) followed by addition of α-ketoester (1 equiv. of methyl, ethyl pyruvate or 1,2-diketone, and excess of phenyl or isobutyl pyruvates). The mixture was left to stir under argon for 1 h after which the UV-visible spectrum showed no starting material, but instead a new product absorbing at 450 and 520 nm. Excess TFA was removed by washing with aqueous Na_2CO_3 (product color changed from reddish to green). The UV-visible absorption for the green product showed peaks at 430 and 790 nm. $Zn(OAc)_2$ (20 mg) dissolved in 1 mL of dry methanol was added to the green product in dry dichloromethane (20 mL) and stirred under argon. The reaction mixture immediately changed color to reddish, and after stirring for 5 min the UV-visible spectrum indicated new absorptions at around 470 and 540 nm. 50 mg (0.22 mmol) of DDQ dissolved in dry dichloromethane (0.3 mL) was added to oxidize the product. After 15 min, the UV-visible spectrum of the mixture showed absorptions at 430 and 840 nm, suggesting formation of a zinc isoporphyrin. The mixture was washed with water, then brine, and dried over anhydrous Na_2SO_4. Purification on an alumina column (Grade III) eluting with dechloromethane separated the main fraction which absorbed at 430 and 830 nm, as expected for a zinc isoporphyrin. Further purification was carried out on silica gel using dichloromethane/ethyl acetate (7:3) to yield a pure product which was further recrystallized using dichloromethane/petroleum ether.

Zinc(II) 2,3,5,7,8,12,13,17,18-nonamethyl-5-methoxycarbonylisoporphyrin chloride (10a)—25 mg, 55% yield. UV-vis (CH_2Cl_2): λ_{max}, nm (ε × 10^4, $M^{-1}.cm^{-1}$) 430 (3.37), 830 (2.63). ^{1}H NMR ($CDCl_3$, 300 MHz): δ, ppm 7.69 (s, *meso*-H, 1H), 7.62 (s, *meso*-H, 2H), 3.73 (s, 5-OCH_3, 3H), 2.58, 2.47, 2.45, 2.42 (s, β-CH_3, 24H), 2.01 (s, 5-CH_3, 3H). HR ESI calcd. for $C_{31}H_{33}N_4O_2Zn$ 557.1889, found *m/z* 557.1895 $[M]^+$. MS (MALDI-TOF): calcd. 559.01, found *m/z* 559.80 $[M]^+$ (dithranol).

Zinc(II) 2,3,5,7,8,12,13,17,18-nonamethyl-5-ethoxycarbonylisoporphyrin chloride (10b)—25 mg, 54% yield. UV-vis (CH_2Cl_2): λ_{max} , nm (ε × 10^4, $M^{-1}.cm^{-1}$) 429 (3.58), 826 (2.89). ^{1}H NMR ($CDCl_3$, 400 MHz): δ, ppm 7.68 (s, *meso*-H, 1H), 7.61 (s, *meso*-H, 2H), 4.10–4.15 (q, OCH_2CH_3, 2H), 2.45, 2.43, 2.40, 2.31 (s, β-CH_3, 24H), 1.96 (s, 5-CH_3, 3H), 1.07–1.04 (t, OCH_2CH_3, 3H). HR ESI calcd. for $C_{32}H_{35}N_4O_2Zn$ 571.2051, found *m/z* 571.2041 $[M]^+$. MS (MALDI-TOF): calcd. 573.04, found *m/z* 573.70 $[M]^+$ (dithranol).

Zinc(II) 5-ethoxycarbonyl-2,3,7,8,12,13,17,18-octamethyl-5-phenylisoporphyrin chloride (10d)—18 mg, 35% yield. UV-vis (CH_2Cl_2): λ_{max}, nm ($\varepsilon \times 10^4$, $M^{-1}.cm^{-1}$) 439 (4.84), 842 (4.27). ^1H NMR ($CDCl_3$, 300 MHz): δ, ppm 8.35, 7.70 (m, 5H, Ph), 7.77 (s, *meso*-H, 1H), 7.66 (s, *meso*-H, 2H), 4.27–4.24 (q, OCH_2CH_3, 2H,), 2.50, 2.44, 2.34, 1.94 (s, β-CH_3, 24H), 1.14 (t, OCH_2CH_3, 3H). HR ESI calcd. for $C_{37}H_{37}N_4O_2Zn$ 633.2207, found *m/z* 633.2202 $[M]^+$. MS (MALDI-TOF): calcd. 635.10, found *m/z* 635.61 $[M]^+$ (dithranol).

Zinc(II) 13,17-diethyl-5-ethoxycarbonyl-5-isobutyl-2,3,7,8,12,18-hexamethylisoporphyrin chloride (10e)—16 mg, 33% yield. UV-vis (CH_2Cl_2): λ_{max}, nm ($\varepsilon \times 10^4$, $M^{-1}.cm^{-1}$) 431 (2.75), 822 (2.28). ^1H NMR ($CDCl_3$, 400 MHz): δ, ppm 7.89 (s, *meso*-H, 1H), 7.80 (s, *meso*-H, 2H), 4.01–3.89 (q, OCH_2CH_3, 2H), 3.04–2.96 (q, -CH_2CH_3, 4H), 2.55, 2.51, 2.43 (s, β-CH_3, 18H), 1.96 (s, 5-CH_3, 3H), 1.32–1.20 (m, –CH_2–CH–, 3H), 1.01–0.96 (t, OCH_2CH_3, 3H), 0.94–0.86 (t, –CH_2CH_3, 6H), 0.44 (d, -CH $(CH_3)_2$, 6H). HR ESI calcd. for $C_{37}H_{45}N_4O_2Zn$ 641.2833, found *m/z* 641.2832 $[M]^+$. MS (MALDI-TOF): calcd. 643.17, found *m/z* 643.56 $[M]^+$ (dithranol).

Zinc(II) 5-acetyl-2,3,5,7,8,12,13,17,18-nonamethylisoporphyrin chloride (10g)—24 mg, 54% yield. UV-vis (CH_2Cl_2): λ_{max}, nm ($\varepsilon \times 10^4$, $M^{-1}.cm^{-1}$) 430 (4.23), 812 (3.87). ^1H NMR ($CDCl_3$, 400 MHz): δ, ppm 8.10 (s, *meso*-H, 1H), 8.07 (s, *meso*-H, 2H), 2.60, 2.57(s, β-CH_3, 24H), 2.30 (s, COMe, 3H), 1.91 (s, 5-CH_3, 3H). HR ESI calcd. for $C_{31}H_{33}N_4OZn$ 541.1940, found *m/z* 541.1943 $[M]^+$. MS (MALDI-TOF): calcd. 543.01, found *m/z* 542.80 $[M]^+$ (dithranol).

2,3,7,8,12,13,17,19-octamethyl-5-phenylporphyrin (11d)—Zinc(II) isoporphyrin (**10d**) was dissolved in dry dichloromethane followed by addition of 5% KOH dissolved in dry methanol. The reaction mixture was left to stir under argon for 1 h after which the color of the mixture turned purple. The UV-visible spectrum indicated no starting material. Excess KOH was neutralized by washing with acetic acid (pH = 5), then with water several times. The organic phase was dried over anhydrous Na_2SO_3, and purified by column chromatography on alumina (Grade III) using dichloromethane as eluent, to give **Zn11d** after evaporation. The product was dissolved in TFA, and allowed to stand at room temperature for 30 min before being poured into water and extracted with dichloromethane. The organic phase was washed with aqueous $NaHCO_3$, the with water, and evaporated to give **11d**, 8 mg, 32% yield. ^1H NMR ($CDCl_3$, 300 MHz): δ, ppm 10.17 (s, *meso*-H, 2H), 9.96 (s, *meso*-H, 1H), 8.10, 7.79 (m, Ph, 5H), 3.65, 3.62, 3.56 (s, β-CH_3, 24H), -3.15 (br, NH, 2H). HR ESI calcd. for $C_{34}H_{34}N_4$ 498.2783, found *m/z* 498.2767 $[M]^+$. MS (MALDI-TOF): calcd. for $C_{34}H_{34}N_4$ 498.28, found *m/z* 498.29 $[M]^+$.

cell studies

Tissue culture—All tissue culture media and reagents were obtained from Invitrogen. The human HEp2 cell line was purchased from ATCC. Cells were maintained in a 50:50 mix of DMEM:Advanced MEM (Gibco) + 5% Fetal Bovine Serum (FBS) (Gibco) in a humidified, 5% CO_2 incubator at 37 °C.

Time dependent cellular uptake—HEp2 cells were seeded at 7500 cells per well in a 96 well plate (Costar) and allowed to attach for 36 h. ZnIP's **6**, **10a**, **10b**, **10d**, **10e**, and **10g** stocks were prepared in DMSO at a concentration of 10 mM and then diluted into medium to final working concentrations. Cells were then exposed to 20 μM of ZnIP in medium for 0, 1, 2, 4, 7, and 24 h. At the end of the loading period, the loading medium was removed; cells were washed with PBS (200 μL), and solubilized with 100 μL 0.25% Triton X100 in PBS. Intercellular accumulation of ZnIP derivatives was determined by measuring the compound's fluorescence emission using a BMG FluoStar Optima plate reader using

excitation/emission wavelengths of 410 nm and 840 ± 40 nm respectively. Cell numbers were measured using the CyQuant Cell Proliferation Assay (Promega).

Cytotoxicity—*Dark toxicity.* HEp2 cells were plated as described above and allowed 36–48 h to grow. Two fold serial dilutions of zinc isoporphyrin **6** and copper isoporphyrin **7** ranging from 0–100 8 μM, and concentrations of 0.0, 2.5, 5.0, 10.0 and 20.0 μM for zinc isoporphyrins **10a**, **10b**, **10d**, **10e**, and **10g** were prepared in the plate and exposed to the cells. After 24 h incubation, the loading medium was removed and viability was determined using Cell Titer Blue Cell Viability Assay Kit (Promega). Results were read using a BMG FluoStar Optima plate reader with an excitation/emission wavelength of 520 nm and 584 nm respectively.

Phototoxicity—HEp2 cells were prepared as per the cytotoxicity experiment. Compound was loaded into the cells and incubated overnight at a concentration range of 0.0, 6.25, 12.5, 25.0, 50.0 and 100.0 μM for zinc isoporphyrin **6** and copper isoporphyrin **7**, and 0.0, 2.5, 5.0, 10.0 and 20.0 μM for zinc isoporphyrins **10a**, **10b**, **10d**, **10e**, and **10g**. Loading medium was then removed and replaced with growth medium containing 50 mM HEPES pH 7.2. Cells were then exposed to light from a 100 Watt halogen light source filtered through a 610 nM long pass filter. To protect cells from overheating, the plate was cooled by placing on a metal block in an ice water bath and IR radiation was filtered by placing 10 mm of water in the light path. Exposure to the light source was the equivalent of 1 $J.cm^{-2}$. After exposure, the cells were incubated overnight and viability was assayed using Cell Titer Blue as in the cytotoxicity assay above.

Fluorescence microscopy—HEp2 cells were seeded onto Lab-Tek II, 2-chamber cover glass and incubated for 48 h. Metallo-isoporphyrins **6**, **7**, **10a**, **10b**, and **10d**, at a concentration of 10 μM, and 2.5 μM for compounds **10e** and **10g** was then added to the cells and incubated for 24 h. The cells were then washed with drug-free medium and fed medium containing 50 mM HEPES pH 7.2. Coverslips were examined using a Zeiss Axiovert 200M inverted fluorescent microscope fitted with standard FITC and Texas Red filter sets (Chroma Technologies). The images were acquired with a Zeiss Axiocam MRM CCD camera fitted to the microscope.

For co-localization experiments, the organelle tracers, MitoTracker Green (mitochondria), LysoSensor Green (lysosomes), ER-Tracker Green (ER), and BODIPY FL C_5-ceramide (Golgi) were introduced into the cells for the final 30 min of incubation concurrently with metalloisoporpyrins, before being washed and prepared for microscopy as described above. Organelle tracers were obtained from Molecular Probes (Invitrogen) and used as per the manufactures instructions.

CONCLUSION

The b-bilene route is shown to be a successful pathway for the synthesis of metallo-isoporphyrins in high yields (28% *vs*. 6% previously reported) and employing a much shorter reaction time (24 h) than previously reported (6 days). Through this route, a novel copper isoporphyrin was obtained. In addition, metal-free and zinc isoporphyrins were isolated and characterized, and could be transformed into their corresponding *meso*-monosubstituted porphyrins. Cell studies show that all metallo-isoporphyrins accumulate within HEp2cells and localize in mitochondria; in addition they were also found in other organelles, including the lysosomes and the ER. The zinc-isoporphyrins were moderately phototoxic (IC_{50} = 11–35 μM at 1 J/cm^2) while the copper-isoporphyrin showed only low cytoxicity (IC_{50} > 85 μM), both in the dark and after exposure to 1 J/cm^2 light dose.

Acknowledgments

This work was supported by grants from the US National Institutes of Health (CA 132861, KMS; CA 139385, MGHV).

REFERENCES

1. Woodward RB. Ind. Chim. Belge. 1962; 27:1293.
2. Dolphin D, Felton RH, Borg DC, Fajer J. J. Am. Chem. Soc. 1970; 92:743.
3. Gold A, Ivey W, Toney GE, Sangaiah R. Inorg. Chem. 1984; 23:2932.
4. Takeda Y, Takahara S, Kobayashi Y, Misawa H, Sakuragi H, Tokumaru K. Chem. Lett. 1990; 11:2103.
5. Harriman A, Porter G, Walters P. J. Chem. Soc., Faraday Trans. 1. 1983; 79:1335.
6. Mosseri S, Mialocq JC, Perly B, Hambright P. J. Phys. Chem. 1991; 95:2196.
7. Richoux M- C, Neta P, Chistensen PA, Harrimann A. J. Chem. Soc., Faraday Trans. 2. 1986; 82:235.
8. Szulbinski W, Strojek JW. J. Electroanal. Chem. Interfacial Electrochem. 1988; 252:323.
9. Araiso T, Miyoshi K-I, Yamazaki I. Biochemistry. 1976; 15:3059. [PubMed: 8081]
10. Ator MA, David SA, Ortiz de Montellano PR. J. Biol. Chem. 1987; 262:14954. [PubMed: 3667617]
11. Morishima I, Ogawa S. Biochemistry. 1978; 17:4384. [PubMed: 568936]
12. Porter DJT, Bright HJ. J. Biol. Chem. 1983; 258:9913. [PubMed: 6885775]
13. Wiseman JS, Nichols JS, Kolpak MX. J. Biol. Chem. 1982; 257:6328. [PubMed: 7076673]
14. Xie H, Smith KM. Tetrahedron Lett. 1992; 33:1197.
15. Xie H, Leung SH, Smith KM. J. Porphyrins Phthalocyanines. 2002; 6:607.
16. Arsenault GP, Bullock E, MacDonald SF. J. Am. Chem. Soc. 1960; 82:4384.
17. Fawcett WR, Fedurco M, Smith KM, Xie H. J. Electroanal. Chem. 1993; 354:281.
18. Barkigia KM, Renner MW, Xie H, Smith KM, Fajer J. J. Am. Chem. Soc. 1993; 115:7894.
19. Gentemann S, Leung SH, Smith KM, Fajer J, Holten D. J. Phys. Chem. 1995; 99:4330.
20. Jackson AH, Kenner GW, Smith KM. J. Chem. Soc. C. 1971:502.
21. Mwakwari, SC. Ph.D. Dissertation. Louisiana State University; 2007.
22. Mwakwari C, Fronczeck FR, Smith KM. Chem. Commun. 2007:2258.
23. Selman SH, Hampton JA, Morgan AR, Keck RW, Balkany AD, Skalkos D. Photochem. Photobiol. 1993; 57:681. [PubMed: 8506398]
24. Hampton JA, Skalkos D, Taylor PM, Selman SH. Photochem. Photobiol. 1993; 58:100. [PubMed: 8378428]
25. Sibrian-Vazquez M, Nesterova IV, Jensen TJ, Vicente MGH. Bioconj. Chem. 2008; 19:705–713.
26. Jensen TJ, Vicente MGH, Luguya R, Norton J, Fronczek FR, Smith KM. J. Photochem. Photobiol., B. 2010; 100:100–111. [PubMed: 20558079]
27. Luo Y, Chang CK, Kessel D. Photochem. Photobiol. 1996; 63:528–534. [PubMed: 8934765]
28. Kessel D, Luo Y. J. Photochem. Photobiol., B. 1998; 42:89–95. [PubMed: 9540214]
29. Kessel D. J. Porphyrins Phthalocyanines. 2004; 8:1009–1014.

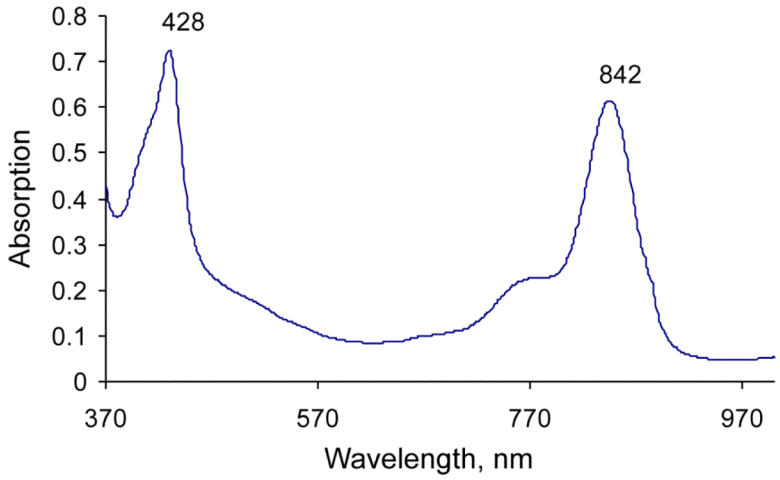

Fig. 1.
UV-visible spectrum of copper isoporphyrin (**7**) in dichloromethane

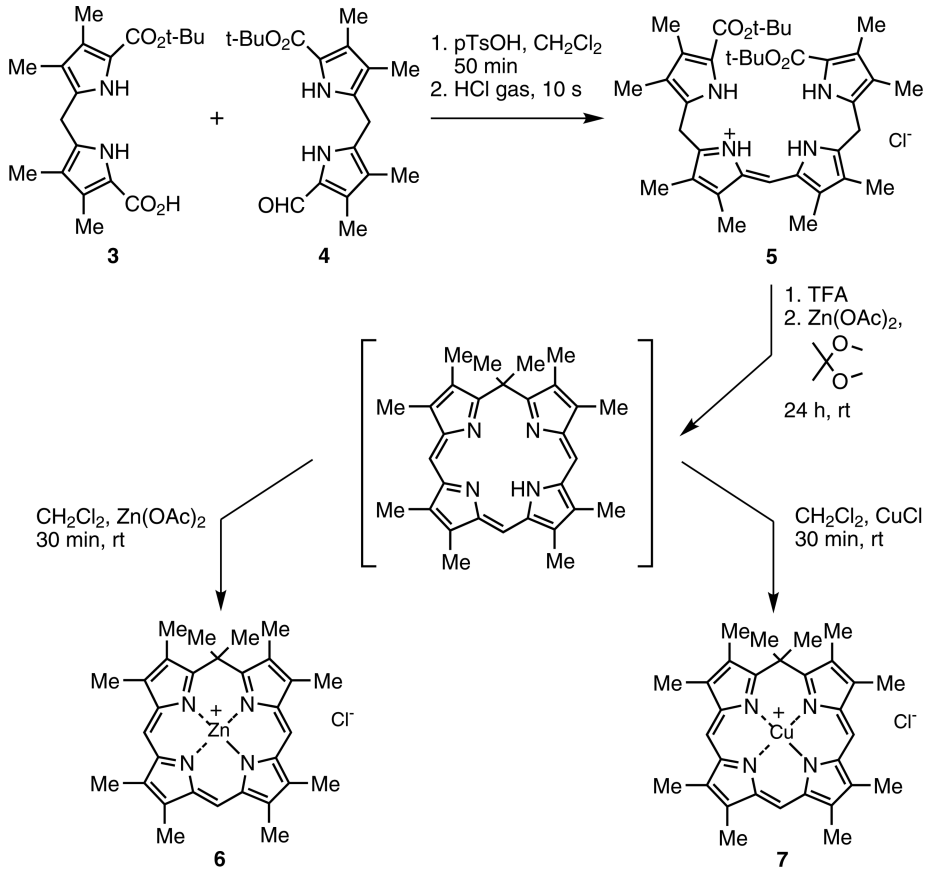

Scheme 1.
Syntheses of zinc (**6**) and copper (**7**) isoporphyrin salts *via* b-bilene (**5**)

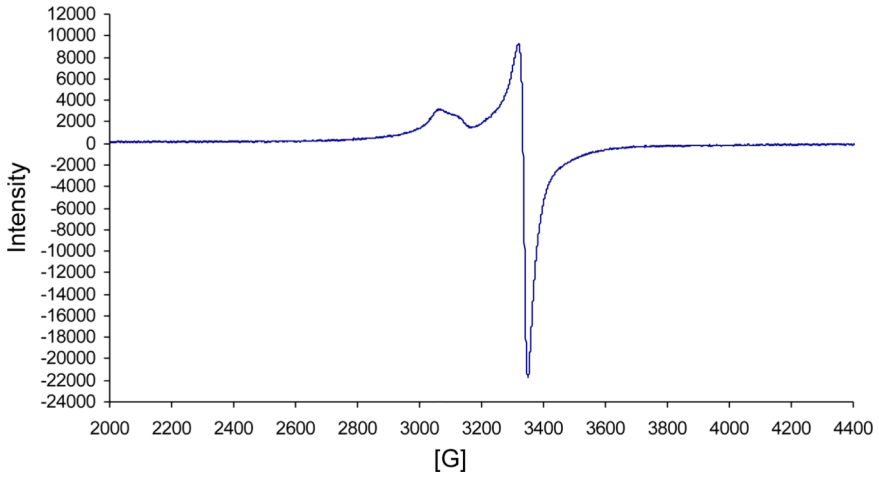

Fig. 2.

WinEPR spectrum of copper(II) isoporphyrin (**7**) in dichloromethane. Frequency: 9.634 GHz, Mod. Frequency: 100.00 kHz, Power: 20.170 mW, Mod. Amplitude: 4.00 G, Temperature: 295 K

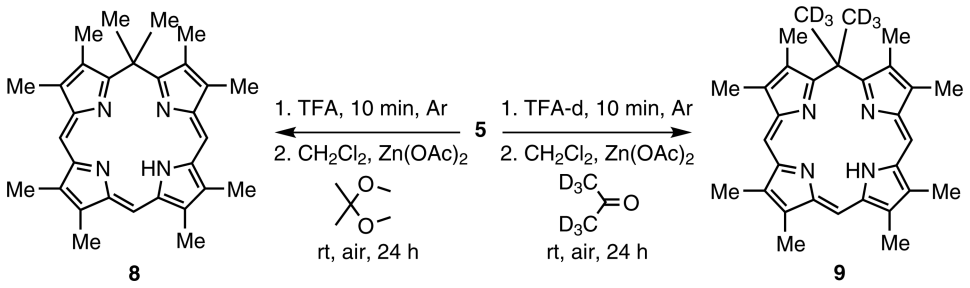

Scheme 2.

Synthesis of metal-free isoporphyrin (**8**) and deuterium labeled metal-free isoporphyrin (**9**)

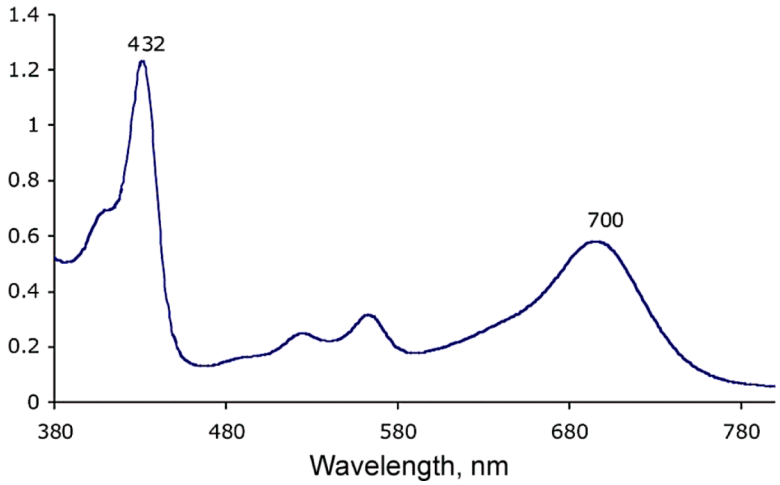

Fig. 3.
UV-visible spectrum of protonated metal-free isoporphyrin (**8**) in dichloromethane

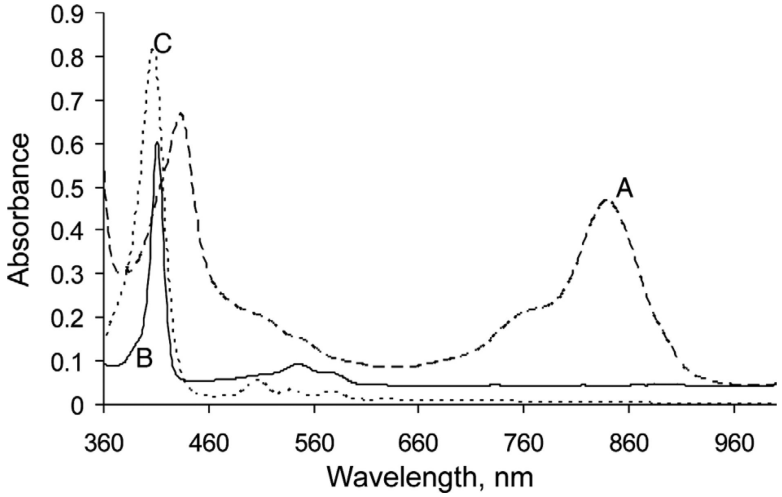

Fig. 4.

Electronic absorption spectra in dichloromethane of: (A) zinc isoporphyrin (**10d**) before (dashed line) and (B) after (full line) after transformation to zinc *meso*-monosubstituted porphyrin (**11d),** and then (C) after demetalation (dotted line)

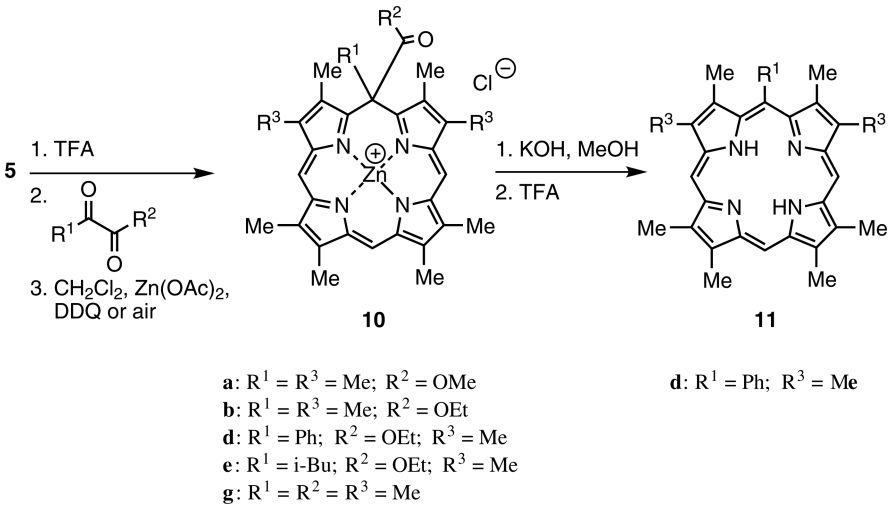

Scheme 3.

Cyclization of b-bilene to isoporphyrins (**10**) followed by transformation to *meso*-monosubstituted porphyrins (**11**)

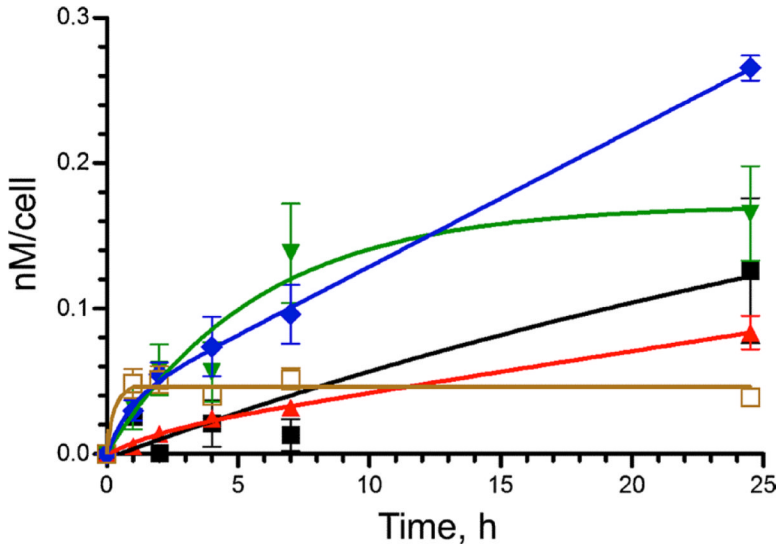

Fig. 5.

Time-dependent cellular uptake of compounds **6** (brown open square), **10a** (black square), **10b** (red triangle), **10d** (green inverted triangle), and **10e** (blue diamond), in HEp2 cells at 20 μM, for 24 h

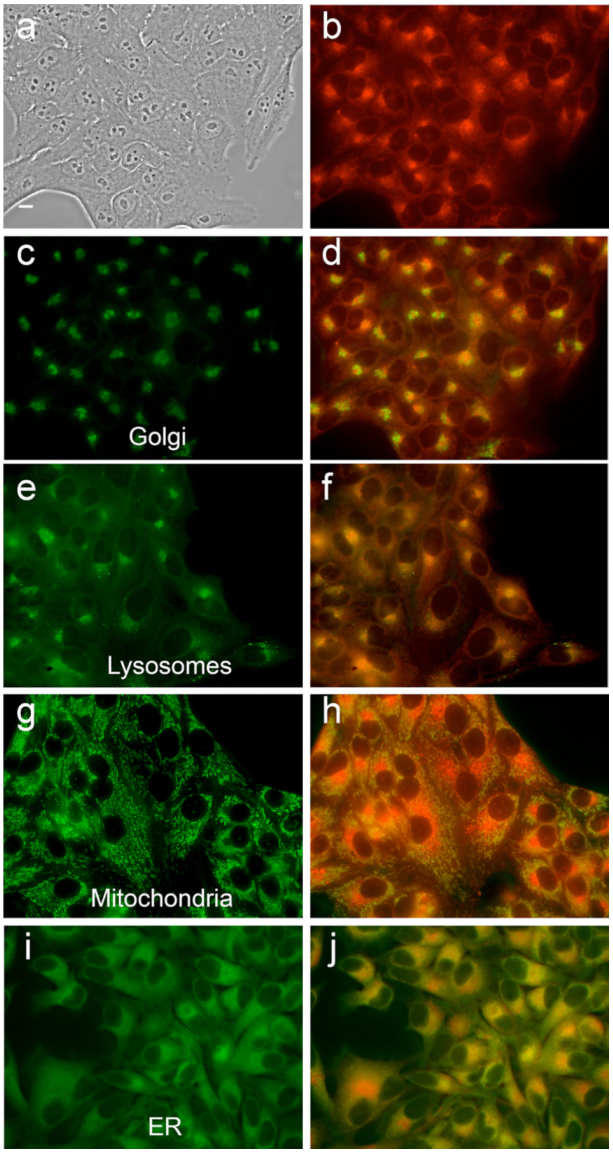

Fig. 6.

Intracellular localization of zinc isoporphyrin (**6**) at 10 μM in HEp2 cells. (a) phase contrast; (b) overlay of phase contrast with fluorescence of zinc isoporphyrin, (**6**); (c, e, g and i) show the fluorescence of BODIPY Ceramide, Lysotracker Green, Mitotracker Green, and ER-Tracker Green, organelle tracers for the Golgi apparatus, lysosomes, mitochondria, and endoplasmic reticulum, respectively; (d, f, h and j) show the overlay of the fluorescence of zinc isoporphyrin (**6**) and the organelle tracers

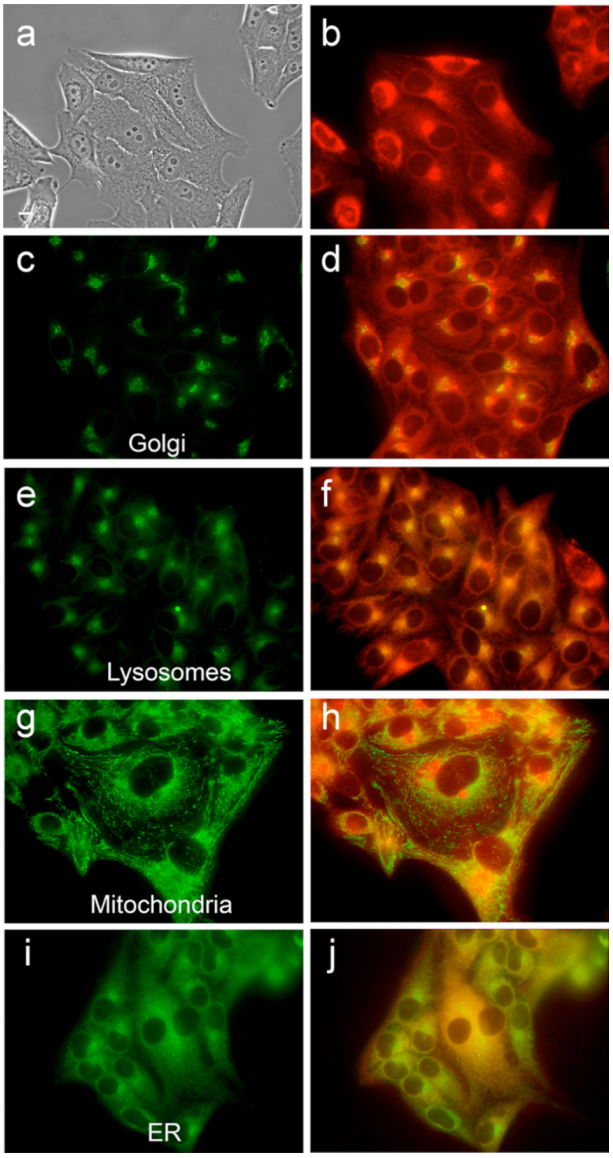

Fig. 7.

Intracellular localization of zinc isoporphyrin (**10a**) at 10 μM in HEp2 cells. (a) phase contrast; (b) overlay of phase contrast with fluorescence of zinc isoporphyrin, (**10a**); (c, e, g and i) show the fluorescence of BODIPY Ceramide, Lysotracker Green, Mitotracker Green, and ER-tracker Green, organelle tracers for the Golgi apparatus, lysosomes, mitochondria, and endoplasmic reticulum, respectively; (d, f, h and j) show the overlay of the fluorescence of zinc isoporphyrin (**10a**) and the organelle tracers

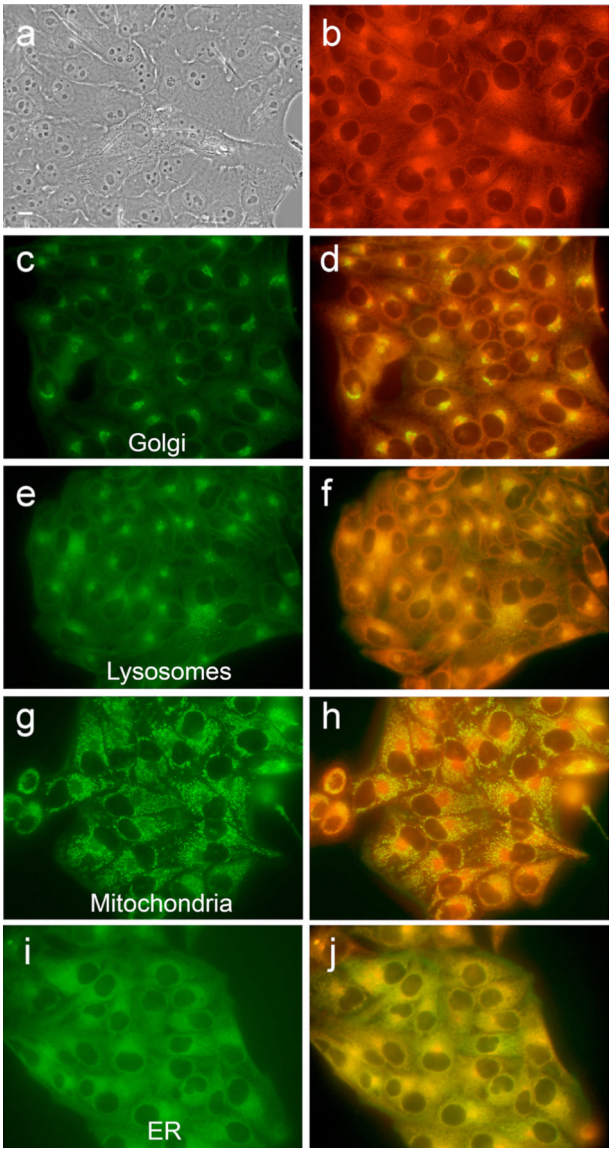

Fig. 8.

Intracellular localization of zinc isoporphyrin (**10b**) at 10 μM in HEp2 cells. (a) phase contrast; (b) overlay of phase contrast with fluorescence of zinc isoporphyrin, (**10b**); (c, e, g and i) show the fluorescence of BODIPY Ceramide, Lysotracker Green, Mitotracker Green, and ER-tracker Green, organelle tracers for the Golgi apparatus, lysosomes, mitochondria, and endoplasmic reticulum, respectively; (d, f, h and j) show the overlay of the fluorescence of zinc isoporphyrin (**10b**) and the organelle tracers

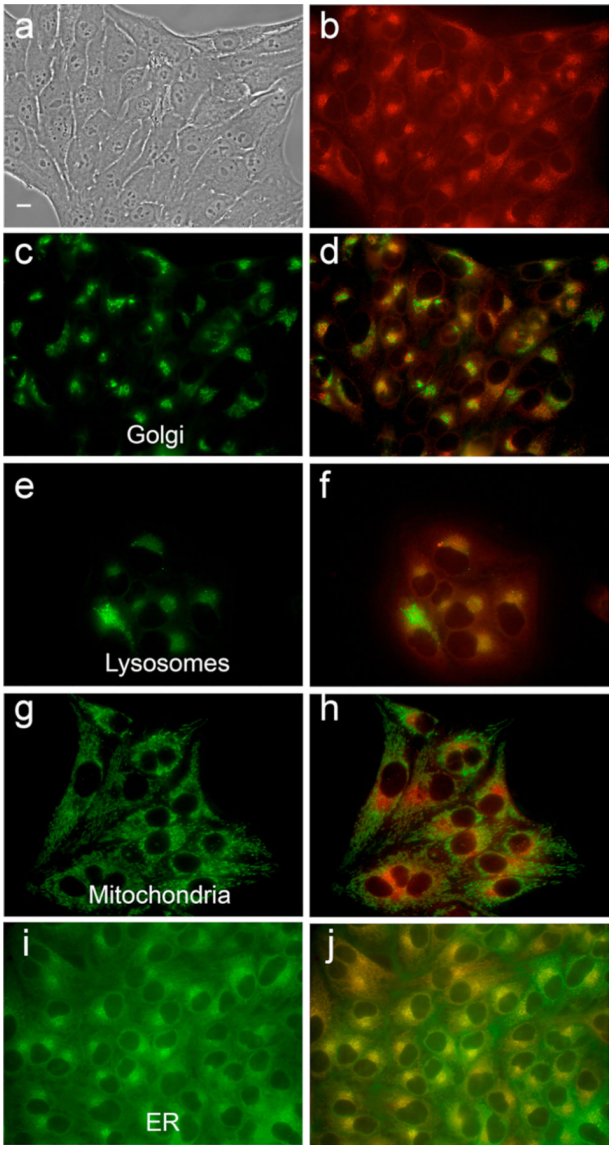

Fig. 9.

Intracellular localization of zinc isoporphyrin (**10d**) at 10 μM in HEp2 cells. (a) phase contrast; (b) overlay of phase contrast with fluorescence of zinc isoporphyrin, (**10d**); (c, e, g and i) show the fluorescence of BODIPY Ceramide, Lysotracker Green, Mitotracker Green, and ER-tracker Green, organelle tracers for the Golgi apparatus, lysosomes, mitochondria, and endoplasmic reticulum, respectively; (d, f, h and j) show the overlay of the fluorescence of zinc isoporphyrin (**10d**) and the organelle tracers

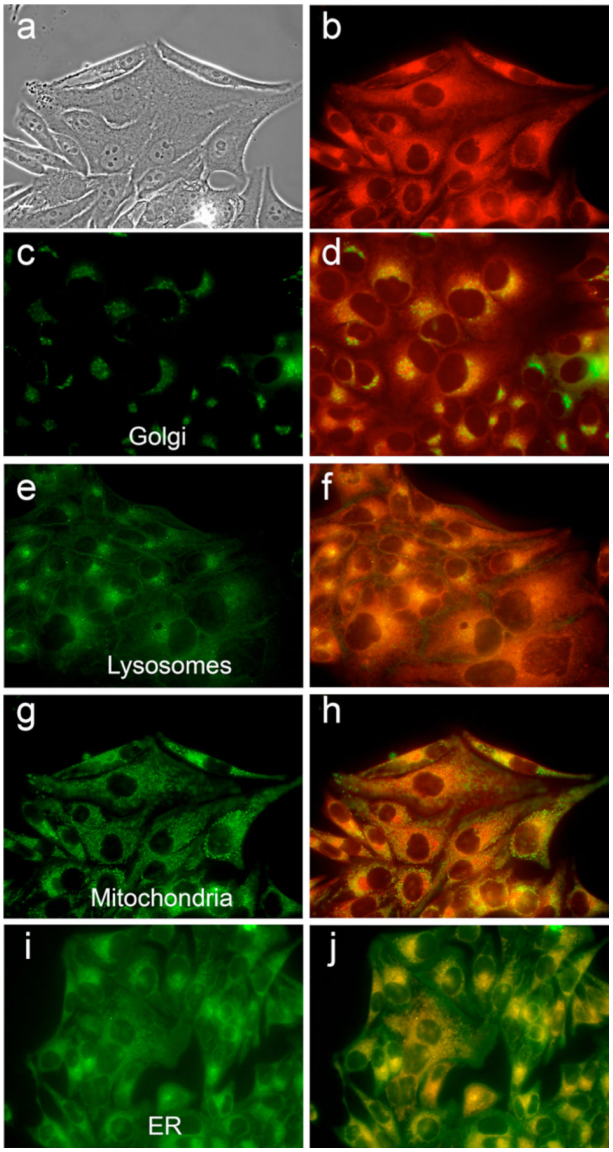

Fig. 10.

Intracellular localization of zinc isoporphyrin (**10e**) at 10 μM in HEp2 cells. (a) phase contrast; (b) overlay of phase contrast with fluorescence of zinc isoporphyrin, (**10e**); (c, e, g and i) show the fluorescence of BODIPY Ceramide, Lysotracker Green, Mitotracker Green, and ER-tracker Green, organelle tracers for the Golgi apparatus, lysosomes, mitochondria, and endoplasmic reticulum, respectively; (d, f, h and j) show the overlay of the fluorescence of zinc isoporphyrin (**10e**) and the organelle tracers

Table 1

Cyclization of b-bilene (5) with various 1,2-diketones to yield zinc isoporphyrin (10)

Cmp	R^1	R^2	Reaction time, min	% yield (10)
10a	Me	OMe	10	55
10b	Me	OEt	10	54
10c	CF_3	OMe	–	0
10d	Ph	OEt	30	35
10e	i-Bu	OEt	60	33
10f	i-Pr	OEt	–	0
10g	Me	Me	10	56

Table 2

Dark toxicity, phototoxicity, and intracellular localization of metallo-isoporphyrins

	Metal ion $[M]^{2+}$	*5,5-geminal* disubstituents R^1, R^2	R^3	Dark toxicity IC_{50}, μM	Phototoxicity IC_{50}, μM	Intracellular localization
6	Zn	Me, Me	Me	85[a]	35	M, L
7	Cu	Me, Me	Me	95[a]	85	M, L
10a	Zn	Me, CO_2Me	Me	≥ 20[b]	17	G, M, L, ER
10b	Zn	Me, CO_2Et	Me	≥ 20[b]	19	G, M, L ER
10d	Zn	Ph, CO_2Et	Me	≥ 20[b]	≥20	L, M, ER
10e	Zn	iBu, CO_2Et	Me	15[b]	11	G, L, M, ER

ER = endoplasmic reticulum; G = Golgi; L = lysosomes; M = mitochondria.

[a]Experiment carried out at concentrations up to: 100 μM

[b]Experiment carried out at concentrations up to: 20 μM.